Inorg. Chem. **2007**, *46*, 3027–3037

Syntheses and Characterization of Six Coordination Polymers of Zinc(II) and Cobalt(II) with 1,3,5-Benzenetricarboxylate Anion and Bis(imidazole) Ligands

Ying-Ying Liu, Jian-Fang Ma,* Jin Yang, and Zhong-Min Su

Key Lab for Polyoxometalate Science, Department of Chemistry, Northeast Normal University, Changchun 130024, People's Republic of China

Received August 21, 2006

Six new coordination polymers, namely $[Zn_{1.5}(BTC)(L^1)(H_2O)_2]\cdot 1.5H_2O$ (**1**), $[Zn_3(BTC)_2(L^2)_3]$ (**2**), $[Zn_3(BTC)_2(L^3)_{1.5}(H_2O)]\cdot H_2O$ (**3**), $[Co_6(BTC)_4(L^1)_6(H_2O)_3]\cdot 9H_2O$ (**4**), $[Co_{1.5}(BTC)(L^2)_{1.5}]\cdot 0.25H_2O$ (**5**), and $[Co_4(BTC)_2(L^3)_2(OH)_2(H_2O)]\cdot 4.5H_2O$ (**6**), where L^1 = 1,2-bis(imidazol-1-ylmethyl)benzene, L^2 = 1,3-bis(imidazol-1-ylmethyl)benzene, L^3 = 1,1′-(1,4-butanediyl)bis(imidazole), and BTC = 1,3,5-benzenetricarboxylate anion, were synthesized under hydrothermal conditions. In **1**–**6**, each of L^1–L^3 serves as a bidentate bridging ligand. In **1**, BTC anions act as tridentate ligands, and compound **1** shows a 2D polymeric structure which consists of 2-fold interpenetrating (6, 3) networks. In compound **2**, BTC anions coordinate to zinc cations as tridentate ligands to form a net with $(6^4\cdot 8^2)_2(8^6)(6^2\cdot 8)_2$ topology. In compound **3**, BTC anions act as tetradentate ligands and coordinate to zinc cations to form a net with $(4\cdot 6^2\cdot 8^3)_2(8\cdot 10^2)(4\cdot 6\cdot 8^3\cdot 10)_2$ topology. In compound **5**, each BTC anion coordinates to three Co cations, and the framework of **5** can be simplified as $(6^4\cdot 8^2)_2(6^2\cdot 8^2\cdot 10^2)(6^3)_2$ topology. For **4** and **6**, the 2D cobalt–BTC layers are linked by bis(imidazole) ligands to form 3D frameworks. In **6**, the Co centers are connected by μ_3-OH and carboxylate O atoms to form two kinds of cobalt–oxygen clusters. Thermogravimetric analyses (TGA) for these compounds are discussed. The luminescent properties for **1**–**3** and magnetic properties for **4**–**6** are also discussed in detail.

Introduction

Current interest in coordination polymers on the basis of the assembly of metal ions and multifunctional organic ligands is rapidly expanding owing to their intriguing architectures and potential applications,[1,2] although rational design and synthesis of metal−organic frameworks (MOFs) with unique structure and function still remains a long-term challenge. The construction of molecular architecture depends on the combination of several factors, like the coordination geometry of metal ions, the nature of organic ligands and counterions, and sometimes the ratio between metal salt and ligand.[3] Thus, understanding how these considerations affect metal coordination and influence crystal packing is at the forefront of controlling coordination supramolecular arrays.

In principle, the exploration of long ligands usually leads to large voids that may further result in interpenetrated or entangled structures,[4] of which the most outstanding ex-

* To whom correspondence should be addressed. E-mail: jianfangma@yahoo.com.cn.

(1) (a) Carlucci, L.; Ciani, G.; Proserpio, D. M.; Sironi, A. *J. Chem. Soc., Dalton Trans.* **1997**, 1801. (b) Hagrman, P. J.; Hagrman, D.; Zubieta, J. *Angew. Chem., Int. Ed.* **1999**, *38*, 2638. (c) Khlobystov, A. N.; Blake, A. J.; Champness, N. R.; Lemenovskii, D. A.; Majouga, A. G.; Zyk, N. V.; Schröer, M. *Coord. Chem. Rev.* **2001**, *222*, 155. (d) Moulton, B.; Zaworotko, M. J. *Chem. Rev.* **2001**, *101*, 1629. (e) Zaworotko, M. J. *Chem. Commun.* **2001**, 1. (f) Yaghi, O. M.; ORKeeffe, M.; Ockwig, N. W.; Chae, H. K.; Eddaoudi, M.; Kim, J. *Nature* **2003**, *423*, 705. (g) Ockwig, N. W.; Delgado-Friederichs, O.; O'Keeffe, M.; Yaghi, O. M. *Acc. Chem. Res.* **2005**, *38*, 176.

(2) (a) Seo, J. S.; Whang, D.; Lee, H.; Jun, S. I.; Oh, J.; Jeon, Y.; Kim, K. *Nature* **2000**, *404*, 982. (b) Halder, G. J.; Kepert, C. J.; Moubaraki, B.; Murray, K. S.; Cashion, J. D. *Science* **2002**, *298*, 1762. (c) Takamizawa, S.; Nakata, E.; Yokoyama, H.; Mochizuki, K.; Mori, W. *Angew. Chem., Int. Ed.* **2003**, *42*, 4331. (d) Dybtsev, D. N.; Chun, H.; Yoon, S. H.; Kim, D.; Kim, K. *J. Am. Chem. Soc.* **2004**, *126*, 32. (e) Kesanli, B.; Cui, Y.; Smith, M. R.; Bittner, E. W.; Bockrath, B. C.; Lin, W. B. *Angew. Chem., Int. Ed.* **2005**, *44*, 72.

(3) (a) Munakata, M.; Wu, L. P.; Kuroda-Sowa, T.; Maekawa, M.; Moriwaki, K.; Kitagawa, S. *Inorg. Chem.* **1997**, *36*, 5416. (b) Suenaga, Y.; Yan, S. G.; Wu, L. P.; Ino, I.; Kuroda-Sowa, T.; Maekawa, M.; Munakata, M. *J. Chem. Soc., Dalton Trans.* **1998**, 1121. (c) Hirsch, K. A.; Wilson, S. R.; Moore, J. S. *Inorg. Chem.* **1997**, *36*, 2960. (d) Carlucci, L.; Ciani, G.; Gudenberg, D. W.; Proserpio, D. M.; Sironi, A. *Chem. Commun.* **1997**, 631. (e) Carlucci, L.; Ciani, G.; Macchi, P.; Proserpio, D. M.; Rizaato, S. *Chem.*—Eur. J. **1999**, *5*, 237.

(4) (a) Batten, S. R.; Robson, R. *Angew. Chem., Int. Ed.* **1998**, *37*, 1460. (b) Wang, X. L.; Qin, C.; Wang, E. B.; Xu, L.; Su, Z. M.; Hu, C. W. *Angew. Chem., Int. Ed.* **2004**, *43*, 5036. (c) Almeida Paz, F. A.; Khimyak, Y. Z.; Bond, A. D.; Rocha, J.; Klinowski, J. *Eur. J. Inorg. Chem.* **2002**, 2823.

10.1021/ic061575l CCC: $37.00
Published on Web 03/15/2007

Chart 1

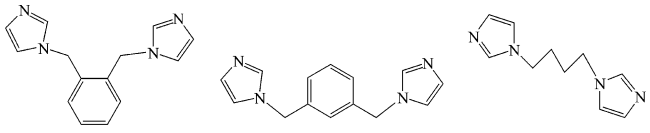

L^1 L^2 L^3

amples are the long dipyridyl ligands, such as 1,2-bis(4-pyridyl)ethane (bpe) and 1,2-di(4-pyridyl)ethylene (dpe). Using these ligands[5] or their mixture with other organic ligands,[6] many desirable interpenetrated metal−organic networks have been constructed. Some studies of metal−organic networks of bis(imidazole)-containing ligands have also been reported.[7] In the previous studies, we reported the syntheses and structures of metal compounds with 1,1′-(1,4-butanediyl)bis(imidazole). The results show that the ligand exhibits a special ability to formulate the compounds, and the results also indicate that different organic anions play an important role in directing the final structures and topologies.[8] To further investigate the influence of the neutral ligands and organic anions on the formation of supramolecular architectures, three bis(imidazole)-containing ligands, 1,2-bis(imidazol-1-ylmethyl)benzene (L^1), 1,3-bis(imidazol-1-ylmethyl)benzene (L^2), and 1,1′-(1,4-butanediyl)bis(imidazole) (L^3) (Chart 1) were chosen as neutral ligands in this work. L^1−L^3 are divergent bidentate ligands with flexible skeletons which contain methylene groups. In the structures of L^1−L^3, the imidazole groups are bridged by different spacers: *o*-xylene (L^1); *m*-xylene (L^2); 1,4-btuyl (L^3). When coordinating to metal centers, the different flexibilities and steric effects of these ligands may diversify the topologies of the networks. 1,3,5-Benzenetricarboxylic acid (H_3BTC) was chosen because the multicarboxylic groups of the molecule may be completely or partially deprotonated, and these anions may act as bridging ligands in various coordination modes.[9] In this paper, we describe the successful syntheses of six new compounds, $[Zn_{1.5}(BTC)(L^1)(H_2O)_2]\cdot 1.5H_2O$ (**1**), $[Zn_3(BTC)_2(L^2)_3]$ (**2**), $[Zn_3(BTC)_2(L^3)_{1.5}(H_2O)]\cdot H_2O$ (**3**), $[Co_6(BTC)_4(L^1)_6(H_2O)_3]\cdot 9H_2O$ (**4**), $[Co_{1.5}(BTC)(L^2)_{1.5}]\cdot 0.25H_2O$ (**5**), and $[Co_4(BTC)_2(L^3)_2(OH)_2(H_2O)]\cdot 4.5H_2O$ (**6**). The crystal structures of these compounds and topological analyses, along with the systematic investigation of the modulated effect of coordination modes of BTC anions and bis(imidazole) ligands on the ultimate framework, will be represented and discussed.

Experimental Section

Materials. All reagents and solvents for syntheses were purchased from commercial sources and used as received. The ligand L^3 was synthesized according to the literature.[8d] The same procedure was used to synthesize the ligands L^1 and L^2 by using corresponding 1,2-bis(chloromethyl)benzene and 1,3-bis(chloromethyl)benzene instead of 1,4-dichlorobutane.

Synthesis of $[Zn_{1.5}(BTC)(L^1)(H_2O)_2]\cdot 1.5H_2O$ (1). A mixture of $ZnCO_3$ (0.056 g, 0.45 mmol), H_3BTC (0.063 g, 0.30 mmol), L^1 (0.107 g, 0.45 mmol), and water (7 mL) was placed in a Teflon reactor (15 mL). The mixture was heated at 160 °C for 4 days, and then it was gradually cooled to room temperature at a rate of 10 °C·h^{-1}. Colorless crystals of **1** were obtained. Yield: 38% based on $ZnCO_3$. Anal. Calcd for $C_{23}H_{24}Zn_{1.5}N_4O_{9.5}$ (M_r = 606.52): C, 45.55; H, 3.99; N, 9.24. Found: C, 45.79; H, 4.18; N, 9.09. IR (cm^{-1}): 3450 (s), 3128 (s), 1624 (s), 1574 (m), 1526 (m), 1441 (m), 1356 (s), 1238 (m), 1111 (m), 1094 (m), 1028 (w), 953(m), 845 (w), 768 (s), 731 (s), 656 (s).

Synthesis of $[Zn_3(BTC)_2(L^2)_3]$ (2). A mixture of $ZnCO_3$ (0.056 g, 0.45mmol), H_3BTC (0.063 g, 0.30 mmol), and L^2 (0.107 g, 0.45 mmol) in water (7 mL) was heated at 180 °C for 3 days. After the mixture was cooled to room temperature at 10 °C·h^{-1}, colorless crystals of **2** were obtained. Yield: 54% based on $ZnCO_3$. Anal. Calcd for $C_{60}H_{48}Zn_3N_{12}O_{12}$ (M_r = 1325.21): C, 54.38; H, 3.65; N, 12.68. Found: C, 54.99; H, 3.85; N, 12.69. IR (cm^{-1}): 3479 (s), 3119 (s), 1626 (s), 1574 (s), 1526 (m), 1504 (m), 1439 (m), 1342 (s), 1248 (m), 1111 (m), 1095 (m), 1032 (w), 953 (m), 768 (s), 733 (s), 656 (m).

Synthesis of $[Zn_3(BTC)_2(L^3)_{1.5}(H_2O)]\cdot H_2O$ (3). A mixture of $Zn(OAc)_2\cdot 2H_2O$ (0.099 g, 0.45mmol), H_3BTC (0.063 g, 0.30 mmol), and L^3 (0.057 g, 0.30 mmol) in water (7 mL) was heated at 150 °C for 3 days, and then it was cooled to room temperature at 10 °C·h^{-1}. Colorless crystals of **3** were obtained in a 36% yield based on $Zn(OAc)_2\cdot 2H_2O$. Anal. Calcd for $C_{33}H_{31}Zn_3N_6O_{14}$ (M_r = 931.75): C, 42.54; H, 3.35; N, 9.02. Found: C, 41.83; H, 3.56; N, 8.77. IR (cm^{-1}): 3447 (s), 3128 (s), 2945 (w), 1624 (s), 1570 (s), 1526 (s), 1437 (s), 1360 (s), 1248 (m), 1117 (s), 1095 (s), 953 (w), 756 (s), 727 (s), 658 (m).

Synthesis of $[Co_6(BTC)_4(L^1)_6(H_2O)_3]\cdot 9H_2O$ (4). A mixture of $CoCO_3$ (0.054 g, 0.45 mmol), H_3BTC (0.063 g, 0.3 mmol), and L^1

(5) (a) Blake, A. J.; Champness, N. R.; Chung, S. S. M.; Li, W. S.; Schröder, M. *Chem. Commun.* **1997**, 1005. (b) Hagrman, D.; Hammond, R. P.; Haushalter, R.; Zubieta, J. *Chem. Mater.* **1998**, *10*, 2091. (c) Batten, S. R.; Harris, A. R.; Jensen, P.; Murray, K. S.; Ziebell, A. *J. Chem. Soc., Dalton Tran.* **2000**, 3829. (d) Knaust, J. M.; Lopez, S.; Keller, S. W. *Inorg. Chim. Acta* **2002**, *324*, 81. (e) Carlucci, L.; Ciani, G.; Proserpio, D. M.; Rizzato, S. *Chem. Commun.* **2000**, 1319. (f) Ghoshai, D.; Maji, T. K.; Mostafa, G.; Lu, T. H.; Chaudhuri, N. R. *Cryst. Growth Des.* **2003**, *3*, 9. (g) Li, X. J.; Cao, R.; Sun, D. F.; Bi, W. H.; Wang, Y. Q.; Li, X.; Hong, M. C. *Cryst. Growth Des.* **2004**, *4*, 775.

(6) (a) Niel, V.; Muoòz, M. C.; Gaspar, A. B.; Galet, A.; Levchenko, G.; Real, J. A. *Chem.*—Eur. J. **2002**, *8*, 2446. (b) Lu, J. Y.; Babb, A. M. *Inorg. Chem.* **2001**, *40*, 3261. (c) Luo, J.; Hong, M.; Wang, R.; Cao, R.; Han, L.; Lin, Z. *Eur. J. Inorg. Chem.* **2003**, 2705.

(7) (a) Carlucci, L.; Ciani, G.; Proserpio, D. M. *Chem. Commun.* **2004**, 380. (b) Carlucci, L.; Ciani, G.; Proserpio, D. M. Spadacini, L. *CrystEngComm* **2004**, *6*, 96. (c) Fan, J.; Slebodnick, C.; Angel, R.; Hanson, B. E. *Inorg. Chem.* **2005**, *44*, 552. (d) Fan, J.; Slebodnick, C.; Troya, D.; Angel, R.; Hanson, B. E. *Inorg. Chem.* **2005**, *44*, 2719. (e) Li, X. J.; Cao, R.; Bi, W. H.; Wang, Y. Q.; Wang, Y. L.; Li, X. *Polyhedron* **2005**, *24*, 2955. (f) Wen, L. L.; Dang, D. B.; Duan, C. Y.; Li, Y. Z.; Tian, Z. F.; Meng, Q. J. *Inorg. Chem.* **2005**, *44*, 7161. (g) Cui, G. H.; Li, J. R.; Tian, J. L.; Bu, X. H.; Batten, S. R. *Cryst. Growth Des.* **2005**, *5*, 1775. (h) Wang, X. Y.; Li, B. L.; Zhu, X.; Gao, S. *Eur. J. Inorg. Chem.* **2005**, 3277. (i) Li, B. L.; Zhu, X.; Zhou, J. H.; Zhang, Y. *J. Coord. Chem.* **2005**, *58*, 271. (j) Li, X. J.; Wang, X. Y.; Gao, S.; Cao, R. *Inorg. Chem.* **2006**, *45*, 1508.

(8) (a) Ma, J. F.; Liu, J. F.; Xing, Y.; Jia, H. Q.; Lin, Y. H. *J. Chem. Soc., Dalton Trans.* **2000**, 2403. (b) Ma, J. F., Liu, J. F.; Liu, Y. C.; Xing, Y.; Jia, Y. Q.; Lin, Y. H. *New J. Chem.* **2000**, *24*, 759. (c) Ma, J. F., Yang, J.; Zheng, G. L.; Li, L.; Liu, J. F. *Inorg. Chem.* **2003**, *42*, 7531. (d) Yang, J.; Ma, J. F.; Liu, Y. Y.; Li, S. L.; Zheng, G. L. *Eur. J. Inorg. Chem.* **2005**, 2174. (e) Yang, J.; Ma, J. F.; Liu, Y. Y.; Ma, J. C.; Jia, H. Q.; Hu, N. H. *Eur. J. Inorg. Chem.* **2006**, 1208.

(9) (a) Yaghi, O. M.; Li, G. M.; Li, H. L. *Nature* **1995**, *378*, 703. (b) Platers, M. J.; Howie, R. A.; Roberts, A. J. *Chem. Commun.* **1997**, 893. (c) Dai, J. C.; Wu, X. T.; Fu, Z. Y.; Cui, C. P.; Hu, S. M.; Du, W. X.; Wu, L. M.; Zhang, H. H.; Sun, R. O. *Inorg. Chem.* **2002**, *41*, 1391. (d) Choi, H. J.; Suh, M. P. *J. Am. Chem. Soc.* **1998**, *120*, 10622. (e) Chen, W.; Wang, J. Y.; Chen, C.; Yue, Q.; Yuan, H. M.; Chen, J. S.; Wang, S. N. *Inorg. Chem.* **2003**, *42*, 944. (f) Yang, J.; Yue, Q.; Li, G. D.; Cao, J. J.; Li, G. H.; Chen, J. S. *Inorg. Chem.* **2006**, *45*, 2857.

Table 1. Crystal and Structure Refinement Data for Compounds **1**−**6**

param	**1**	**2**	**3**
formula	$C_{23}H_{24}Zn_{1.50}N_4O_{9.50}$	$C_{60}H_{48}Zn_3N_{12}O_{12}$	$C_{33}H_{31}Zn_3N_6O_{14}$
fw	606.52	1325.21	931.75
space group	$P\bar{1}$	Cc	$P\bar{1}$
a (Å)	10.230(8)	40.364(8)	9.316(8)
b (Å)	10.886(8)	8.341(8)	13.670(12)
c (Å)	12.657(10)	18.743(10)	16.355(14)
α (deg)	109.794(14)	90	70.022(13)
β (deg)	105.790(14)	112.685(10)	74.565(13)
γ (deg)	95.411(14)	90	83.573(15)
V (Å^3)	*1249(2)*	*5822(6)*	*1886(3)*
Z	2	4	2
D_{calcd} (g cm^{-3})	1.613	1.512	1.640
F(000)	622	2664	961
reflcns collcd/unique	7767/5591	26 775/12 640	11 561/8376
GOF on F^2	1.041	1.031	0.920
R_1[a] [$I > 2\sigma(I)$]	0.0546	0.0411	0.0413
wR_2[b]	0.1322	0.0804	0.1022

param	**4**	**5**	**6**
formula	$C_{120}H_{120}Co_6N_{24}O_{36}$	$C_{30}H_{24.5}Co_{1.5}N_6O_{6.25}$	$C_{38}H_{47}Co_4N_8O_{19.5}$
fw	2827.98	657.45	1163.55
space group	$P\bar{1}$	$C2/c$	$P\bar{1}$
a (Å)	16.070(4)	15.942(7)	11.074(2)
b (Å)	19.567(4)	12.172(4)	11.462(2)
c (Å)	22.659(4)	30.831(9)	18.048(4)
α (deg)	74.255(7)	90	83.61(3)
β (deg)	80.665(8)	99.478(5)	84.85(3)
γ (deg)	67.870(7)	90	73.03(3)
V (Å^3)	*6338(2)*	*5901(3)*	*2173.7(8)*
Z	2	8	2
D_{calcd} (g cm^{-3})	1.482	1.480	1.776
F(000)	2916	2696	1188
reflcns collcd/unique	61 708/27 867	27 689/6628	20 960/9575
GOF on F^2	1.018	0.962	1.103
R_1[a] [$I>2\sigma$ (I)]	0.0627	0.0769	0.0661
wR_2[b]	0.1711	0.1940	0.1956

[a] $R_1 = \sum||F_o| - |F_c||/\sum|F_o|$. [b] $wR_2 = |\sum w(|F_o|^2 - |F_c|^2)|/\sum|w(F_o^2)^2|^{1/2}$.

(0.107 g, 0.45 mmol) in water (8 mL) was heated at 160 °C for 4 days, and then it was cooled to room temperature at 10 °C·h^{-1}. Purple crystals of **4** were obtained in a 76% yield based on $CoCO_3$. Anal. Calcd for $C_{120}H_{120}Co_6N_{24}O_{36}$ (M_r = 2827.98): C, 50.97; H, 4.28; N, 11.89. Found: C, 51.21; H, 4.35; N, 11.91. IR (cm^{-1}): 3445 (s), 3130 (s), 1722 (m), 1622 (s), 1558 (s), 1443 (m), 1387 (s), 1234 (m), 1153 (w), 1111 (m), 1090 (m), 937 (s), 829 (w), 762 (s), 725 (s), 658 (s).

Synthesis of $[Co_{1.5}(BTC)(L^2)_{1.5}]\cdot 0.25H_2O$ (5). A mixture of $CoCO_3$ (0.054 g, 0.45 mmol), H_3BTC (0.095 g, 0.45 mmol), and L^2 (0.107 g, 0.45 mmol) in water (7 mL) was heated at 180 °C for 3 days, and then it was slowly cooled to room temperature at 10 °C·h^{-1}. Purple crystals of **5** were obtained in a 70% yield based on $CoCO_3$. Anal. Calcd for $C_{30}H_{24.5}Co_{1.5}N_6O_{6.25}$ (M_r = 657.45): C, 54.81; H, 3.76; N, 12.78. Found: C, 54.88; H, 3.79; N, 12.90. IR (cm^{-1}): 3440 cm^{-1} (s), 3214 (m), 2845 (w), 1626 (s), 1439 (m), 1342 (m), 1241 (s), 1092 (s), 767 (m), 729 (m), 658 (w).

Synthesis of $[Co_4(BTC)_2(L^3)_2(OH)_2(H_2O)]\cdot 4.5H_2O$ (6). A mixture of $CoCO_3$ (0.054 g, 0.45 mmol), H_3BTC (0.063 g, 0.30 mmol), and L^3 (0.085 g, 0.45 mmol) in water (7 mL) was heated at 130 °C for 4 days, and then it was slowly cooled to room temperature at 10 °C·h^{-1}. Purple crystals of **6** were obtained in a 78% yield based on $CoCO_3$. Anal. Calcd for $C_{38}H_{47}Co_4N_8O_{19.5}$ (M_r = 1163.55): C, 39.23; H, 4.07; N, 9.63. Found: C, 39.70; H, 3.96; N, 9.91. IR (cm^{-1}): 3396 cm^{-1} (s), 3126 (s), 2945 (m), 1616 (s), 1558 (s), 1521 (s), 1437 (s), 1364 (s), 1232 (m), 1091 (s), 1033 (w), 941 (w), 837 (m), 768 (s), 725 (s), 660 (s).

General Characterization and Physical Measurements. The C, H, and N elemental analysis was conducted on a Perkin−Elmer 240C elemental analyzer. The FT-IR spectra were recorded from KBr pellets in the range 4000−400 cm^{-1} on a Mattson Alpha-Centauri spectrometer. TGA was performed on a Perkin−Elmer TG-7 analyzer heated from 35 to 800 °C under nitrogen. The luminescent properties of compounds **1**−**3** were measured on a Perkin-Elmer LS55 spectrometer. Temperature-dependent magnetic susceptibility data for polycrystalline compounds **4**−**6** were obtained on a Quantum Design MPMSXL SQUID magnetometer under an applied field of 1000 Oe over the temperature range of 2−300 K.

X-ray Crystallography. Single-crystal X-ray diffraction data for compounds **1** and **2** were recorded on a Bruker Apex CCD diffractometer with graphite-monochromated Mo Kα radiation (λ = 0.710 73 Å) at 293 K. The diffraction data for compounds **3**−**6** were collected on a Rigaku RAXIS-RAPID single-crystal diffractometer with Mo Kα radiation (λ = 0.710 73 Å) at 293 K. Absorption corrections were applied using multiscan technique. All the structures were solved by Direct Method of SHELXS-97[10] and refined by full-matrix least-squares techniques using the SHELXL-97 program.[11] Non-hydrogen atoms were refined with anisotropic temperature parameters. The disordered L^2 ligand in compound **5** was refined using isotropic C and N atoms split over two sites, with a total occupancy of 1. The hydrogen atoms of the organic ligands were refined as rigid groups. Some of the water H atoms in compounds **4**−**6** could not be positioned reliably. Other H atoms

(10) Sheldrick, G. M. *SHELXS-97, Programs for X-ray Crystal Structure Solution*; University of Göttingen: Göttingen, Germany, 1997.
(11) Sheldrick, G. M. *SHELXL-97, Programs for X-ray Crystal Structure Refinement*; University of Göttingen: Göttingen, Germany, 1997.

Structure description of 1.

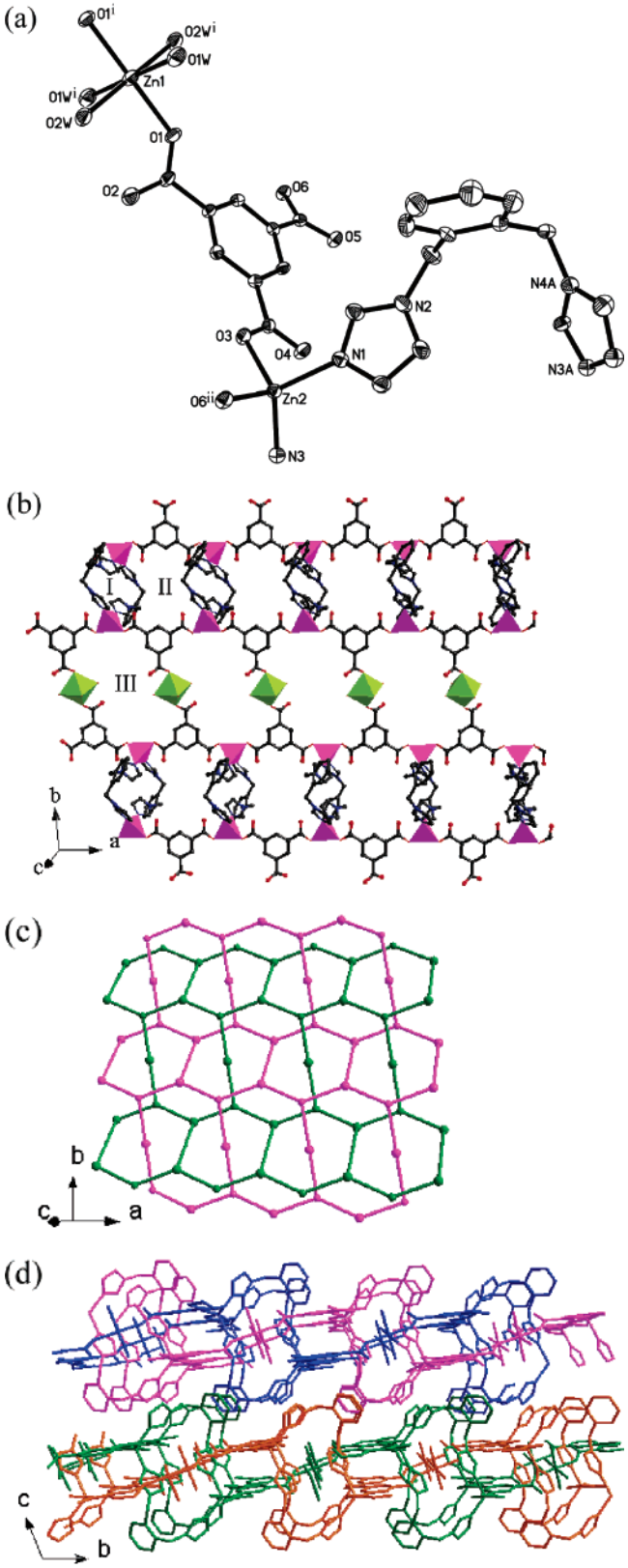

Figure 1. (a) ORTEP diagram showing the coordination environments for Zn atoms in **1**. (b) Infinite 2D network. (c) 2-fold interpenetrating layers of (6, 3) topology. (d) View of the stacking of 2-fold interpenetrating layers.

of water molecules were located from difference Fourier maps. The detailed crystallographic data and structure refinement parameters for **1**−**6** are summarized in Table 1.

Table 2. Hydrogen-Bond Geometries for **1** and **6** (in Å and deg)

D−H···A	*d*(D−H)	*d*(H···A)	*d*(D···A)	<(D−H···A)
Compound **1**				
O(1W)−H(1A)···O(5)^{i}	0.87(3)	1.92(3)	2.784(5)	171(6)
O(1W)−H(1B)···O(4W)^{i}	0.87(3)	1.95(3)	2.809(8)	171(7)
O(2W)−H(2B)···O(2)	0.91(3)	1.79(3)	2.636(6)	153(5)
Compound **6**				
O(5W)−H(5B)···O(8)	0.97(9)	2.05(11)	2.96(1)	156(14)
O(2W)−H(2B)···O(5W)	0.91(8)	2.00(9)	2.86(2)	159(14)

[a] Symmetry codes used to generate equivalent atoms: (i) $-x + 2$, $-y$, $-z + 1$.

Results and Discussion

Syntheses of the Compounds. Hydrothermal synthesis is a relatively complex process, and the final products under a given set of conditions are often unpredictable. The stoichiometry of starting materials is important for the crystal growth of the compounds. The reaction mixtures can produce crystals with M^{II}:H_3BTC = 1.5:1 for **1**−**4** and **6** and M^{II}:H_3BTC = 1:1 for **5** while other stoichiometries fail to produce suitable crystals. However, the isolation of all the compounds is not very sensitive to the content of bis(imidazole) ligands. All crystals were obtained by cooling the reaction system at a rate of 10 °C/h. If the reaction system was cooled to room temperature unaided, no suitable crystals of compounds **1**−**5** could be isolated. In addition, the increase of reaction time can improve the yields of compounds **4** and **6**. All compounds are stable in air and are insoluble in common solvents such as ethanol, benzene, acetone, and acetonitrile. The phase purities of the bulk samples were identified by X-ray powder diffraction (Figures S1−S6 in the Supporting Information).

Structure Description of 1. Selected bond distances and angles for compounds **1**−**6** are listed in Tables S1−S6 (see the Supporting Information). Part of the structure for compound **1** is shown in Figure 1a. There are two kinds of crystallographically unique Zn centers in the structure. Zn1 cation lies at an inversion center and is six-coordinated by four water molecules in the equatorial positions (Zn−O 2.116(4)−2.218(4) Å) and two oxygen atoms from BTC ligands in the axial positions (Zn−O 2.026(3) Å). Zn2 is four-coordinated by two carboxylate oxygen atoms from two BTC anions (Zn−O 1.979(3)−2.000(3) Å) and two nitrogen atoms (Zn−N 2.002(4)−2.017(4) Å) from two L^1 ligands. The Zn−O (carboxylate and water) bond lengths and the Zn−N bond lengths are all within the normal ranges.[12] Each BTC anion in **1** coordinates to three Zn atoms as shown in Chart 2a. The L^1 ligand adopts a cis conformation[13a,b] and coordinates to two Zn centers.

In the structure of **1**, Zn ions are bridged by BTC anions and L^1 ligands to form a 2D polymeric network (Figure 1b).

(12) (a) Majumder, A.; Shit, S.; Choudhury, C. R.; Batten, S. R.; Pilet, G.; Luneau, D.; Daro, N.; Sutter, J. P.; Chattopadhyay, N.; Mitra, S. *Inorg. Chim. Acta* **2005**, *358*, 3855. (b) Zhao, W.; Fan, J.; Okamura, T.; Sun, W. Y.; Ueyama, N. *J. Solid State Chem.* **2004**, *177*, 2358.

(13) (a) Tan, H. Y.; Zhang, H. X.; Ou, H. D.; Dang, B. S. *Inorg. Chim. Acta* **2004**, *357*, 869. (b) Fan, J.; Yee, G. T.; Wang, G. B.; Hanson, B. E. *Inorg. Chem.* **2006**, *45*, 599. (c) Cai, Y. P.; Su, C. Y.; Zhang, H. X.; Zhou, Z. Y.; Zhu, L. X.; Chan, A. S. C.; Liu, H. Q.; Kang, B. S. *Z. Anorg. Allg. Chem.* **2002**, *628*, 2321.

Chart 2. Coordination Modes of BTC Anions in **1**−**6**, $[Zn_3(BTC)_2(H_2O)_8]\cdot 4H_2O$,[12a] and $[Co_3(BTC)_2(H_2O)_{12}]$[24]

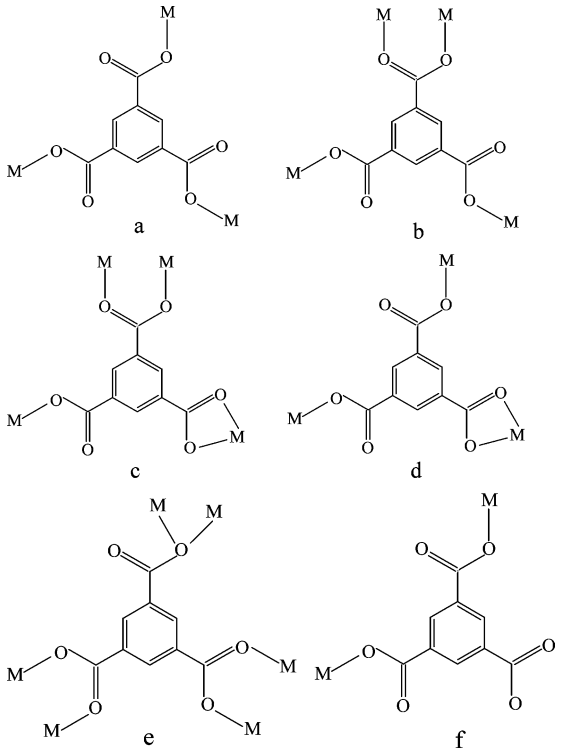

There exist three kinds of rings in this network: Ring I is composed of two Zn2 centers and two L^1 ligands, ring II contains four Zn2 centers, two BTC anions, and two L^1 ligands, and ring III consists of four Zn centers (two Zn1 and two Zn2) and four BTC anions.

If two L^1 ligands coordinated to the same Zn2 center is considered as a connecter, and the BTC anion was considered as a three-connected node, there exist two kinds of three-connected nodes in the framework of **1** (Zn2 center and BTC anion). The topology of this 2D network can thus be described by a (6, 3) net.[14] Twofold interpenetration of these (6, 3) nets occurs in **1** (Figure 1c). As often observed in interpenetrated network structures, close $\pi-\pi$ contacts occur between aromatic rings of BTC anions (with face-to-face distances of 3.40 Å and centroid-to-centriod distance of 3.75 Å). In addition, the interaction between the two interlocked networks is also strengthened by the hydrogen bonds (Table 2 and Figure S7).

As shown in Figure 1d, the overall structure of **1** is obtained by parallel packing of these double-interpenetrating layers. Structural cohesion is achieved by $\pi-\pi$ contacts between the phenyl rings of L^1 ligands of adjacent layers with face to face distances of 3.52 Å and centroid to centriod distances of 3.94 Å.

Structure Description of 2. As illustrated in Figure 2a, the structure of **2** contains three kinds of unique Zn atoms, two kinds of unique BTC anions, and three kinds of unique

(14) (a) Batten, S. R.; Hoskins, B. F.; Robson, R. *New J. Chem.* **1998**, *22*, 173. (b) Chow, Y. M.; Britton, D. *Acta Crystallogr.* **1974**, *B30*, 1117. (c) Schwarten, M.; Chomic, J.; Cernak, J.; Babel, D. *Z. Anorg. Allg. Chem.* **1996**, *622*, 1449. (d) Carlucci, L.; Ciani, G.; Proserpio, D. M.; Sironi, A. *Angew. Chem., Int. Ed. Engl.* **1996**, *35*, 1088.

Structure description of 2.

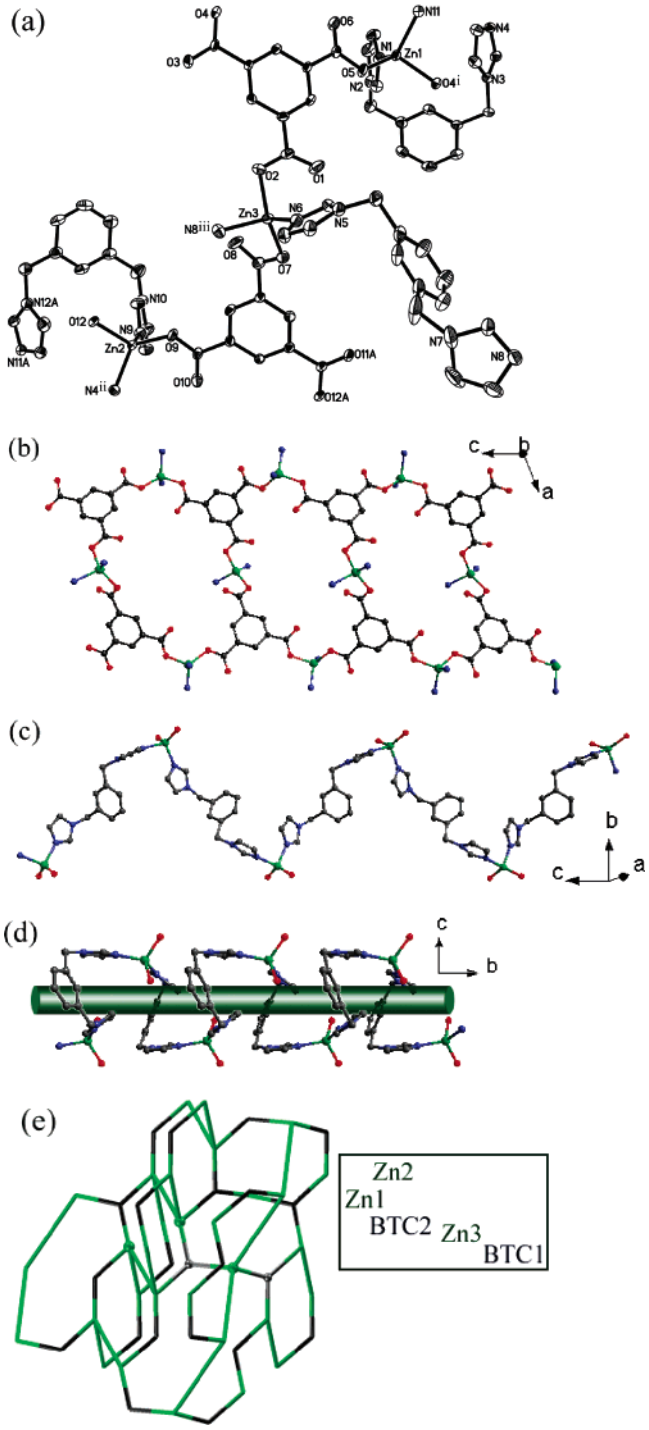

Figure 2. (a) ORTEP view of **2** showing 30% thermal probability ellipsoids. (b) View of the $[Zn_3(BTC)_2]_n$ ladder. (c) Infinite zigzag chain of the S-shaped L^2 ligands. (d) Helical chain of the "C"-shaped L^2 ligands. (e) Schematic diagram (OLEX) showing the $(6^4\cdot 8^2)_2(8^6)(6^2\cdot 8)_2$ network.

L^2 ligands. Each Zn^{II} ion is coordinated by two carboxylate oxygen atoms from two BTC anions (Zn−O 1.929(3)−1.971(3) Å) and two nitrogen atoms from two L^2 ligands (Zn−N 1.987(3)−2.039(2) Å). Each BTC anion coordinates to three Zn^{II} centers (Chart 2a). Zinc cations are bridged by the BTC anions to form a 1D ladder structure (Figure 2b).

Three crystallographically distinct L^2 ligands in **2** adopt two kinds of conformations. One is a S-shaped conforma-

Structure description of 3.

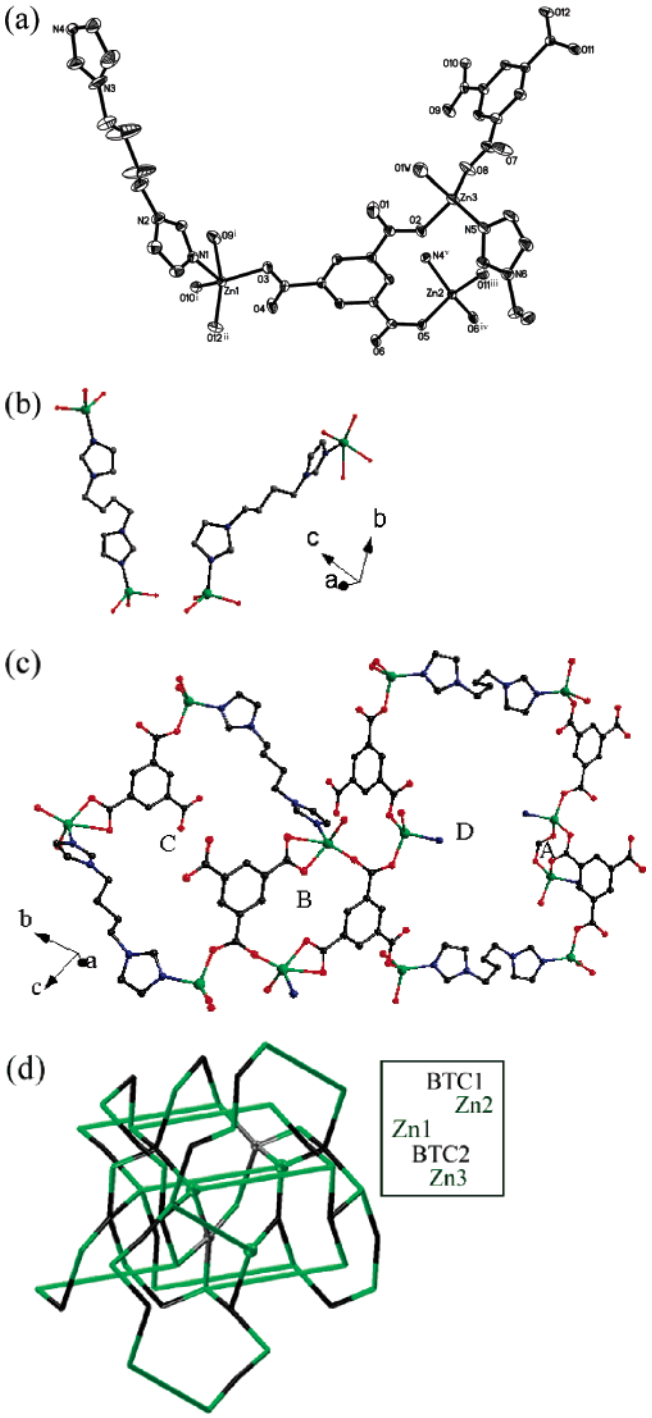

Figure 3. (a) ORTEP diagram showing the coordination environments for zinc atoms in **3**. (b) Different conformations of L^3 ligands in **3**. (c) Network of **3** containing 8-membered (A), 16-membered (B), 38-membered (C), and 54-membered (D) rings. (d) Schematic diagram (OLEX) showing the $(4\cdot6^2\cdot8^3)_2(8\cdot10^2)(4\cdot6\cdot8^3\cdot10)_2$ network.

tion,[15] with Zn···Zn distance of 13.83(5) Å. Each S-shaped L^2 molecule coordinates to two Zn3 cations, acting as a bridging ligand to form an infinite zigzag chain structure (Figure 2c). The $[Zn_3(BTC)_2]$ ladders are extended by these zigzag chains to form a 2D network (Figure S8). The other two kinds of L^2 ligands display C-shaped conformations,[16] with Zn···Zn distances of 7.30(2) and 7.42(2) Å. The alternating arrangement of these two kinds of C-shaped L^2 ligands along the *b*-axis results in a helix (Figure 2d). The 2D networks (Figure S8) are further extended by these helices to produce the complicated 3D polymeric structure of **2**.

If BTC anions are considered as three-connected nodes, the structure of **2** can be simplified to a unique (4, 3)-connected net with $(6^4\cdot8^2)_2(8^6)(6^2\cdot8)_2$ topology (Figures 2e and S9).[17]

Structure Description of 3. Part of the structure for compound **3** is shown in Figure 3a. The structure of **3** contains three kinds of unique Zn atoms, two kinds of unique BTC anions, and two kinds of unique L^3 ligands. The three unique Zn atoms exhibit three different coordination geometries. Zn1 is coordinated by four carboxylate oxygen atoms from three BTC anions (Zn−O 1.964(2)−2.458(3) Å) and one nitrogen atom from L^3 ligand (Zn−N 2.028(3) Å), showing a trigonal bipyramidal geometry.[8a,18] Zn2 is four-coordinated by three carboxylate oxygen atoms from three different BTC anions (Zn−O 1.934(2)−1.984(2) Å) and one nitrogen atom from L^3 ligand (Zn−N 1.978(3) Å). Zn3 atom is four-coordinated by two carboxylate oxygen atoms from two BTC anions (Zn−O 1.947(3)−1.951(2) Å), one N atom from L^3 ligand (Zn−N 1.971(3) Å), and one water molecule (Zn−O 1.998(3) Å).

In compound **3**, the BTC anions display two coordination modes (Chart 2b,c), and each BTC anion coordinates to four Zn^{II} centers. The L^3 ligands in **3** show two distinct conformations with different Zn···Zn distances of 13.44(4) and 12.93(4) Å (Figure 3b). These coordination features have been observed in $[Zn_2(BDC)_2L_2]\cdot2H_2O$ containing a related ligand 1,4-bis(1,2,4-triazol-1-yl)butane.[19] If unique BTC1 anion (containing O1−O6) or BTC2 anion (containing O7−O12) is neglected, two kinds of 2D networks result (Figures S10 and S11). These two kinds of 2D networks cross-link each other to generate a 3D extended network.

As shown in Figure 3c, the zinc centers are bridged by the L^3 ligands and BTC anions to result in four types of rings. Two Zn^{II} centers are linked by BTC anions to form 8-membered (A) and 16-membered (B) rings. Four zinc

(15) (a) Sun, W. Y.; Fan, J.; Okamura, T.; Ueyama, N. *Inorg. Chem. Commun.* **2000**, *3*, 541. (b) Sui, B.; Fan, J.; Okamura, T.; Sun, W. Y.; Ueyama, N. *New J. Chem.* **2001**, *25*, 1379.

(16) (a) Sui, B.; Fan, J.; Okamura, T.; Sun, W. Y.; Ueyama, N. *Solid State Sci.* **2005**, *7*, 969. (b) Sui, B.; Zhao, W.; Ma, G. H.; Okamura, T.; Fan, J.; Li, Y. Z.; Tang, S. H.; Sun, W. Y.; Ueyama, N. *J. Mater. Chem.* **2004**, *14*, 1631. (c) Fan, J.; Sun, W. Y.; Okamura, T.; Zheng, Y. Q.; Sui, B.; Tang, W. X.; Ueyama, N. *Cryst. Growth Des.* **2004**, *4*, 579.

(17) (a) Wells, A. F. *Three-dimensional Nets and Polyhedra*; Wiley-Interscience: New York, 1977. (b) Wells, A. F. *Further Studies of Three-Dimensional Nets;* ACA Monograph 8; American Crystallographic Association: New York, 1979. (c) Dolomanov, O. V.; Blake, A. J.; Champness, N. R.; Schröder, M. *J. Appl. Crystallogr.* **2003**, *36*, 1283. (d) Guo, X. D.; Zhu, G. S.; Li, Z. Y.; Chen, Y.; Li, X. T.; Qiu, S. L. *Inorg. Chem.* **2006**, *45*, 4065.

(18) (a) Wang, X. L.; Qin, C.; Wang, E. B.; Su, Z. M.; Xu, L.; Batten, S. R. *Chem. Commun.* 2005, 4789. (b) Zhang, C. G.; Yu, K. B.; Wu, D.; Zhao, C. X. *Acta Crystallogr.* 1999, *C55*, 1470. (c) Korupoju, S. R.; Mangayarkarasi, N.; Ameerunisha, S.; Valenta, E. J.; Zacharias, P. S. *J. Chem. Soc., Dalton Trans.* 2000, 2845. (d) Muller, B.; Vahrenkamp, H. *Eur. J. Inorg. Chem.* 1999, 137.

(19) Wang, X. L.; Qin, C.; Wang, E. B.; Su, Z. M. *Chem.*—Eur. J. **2006**, *10*, 2680.

Structure description of 4.

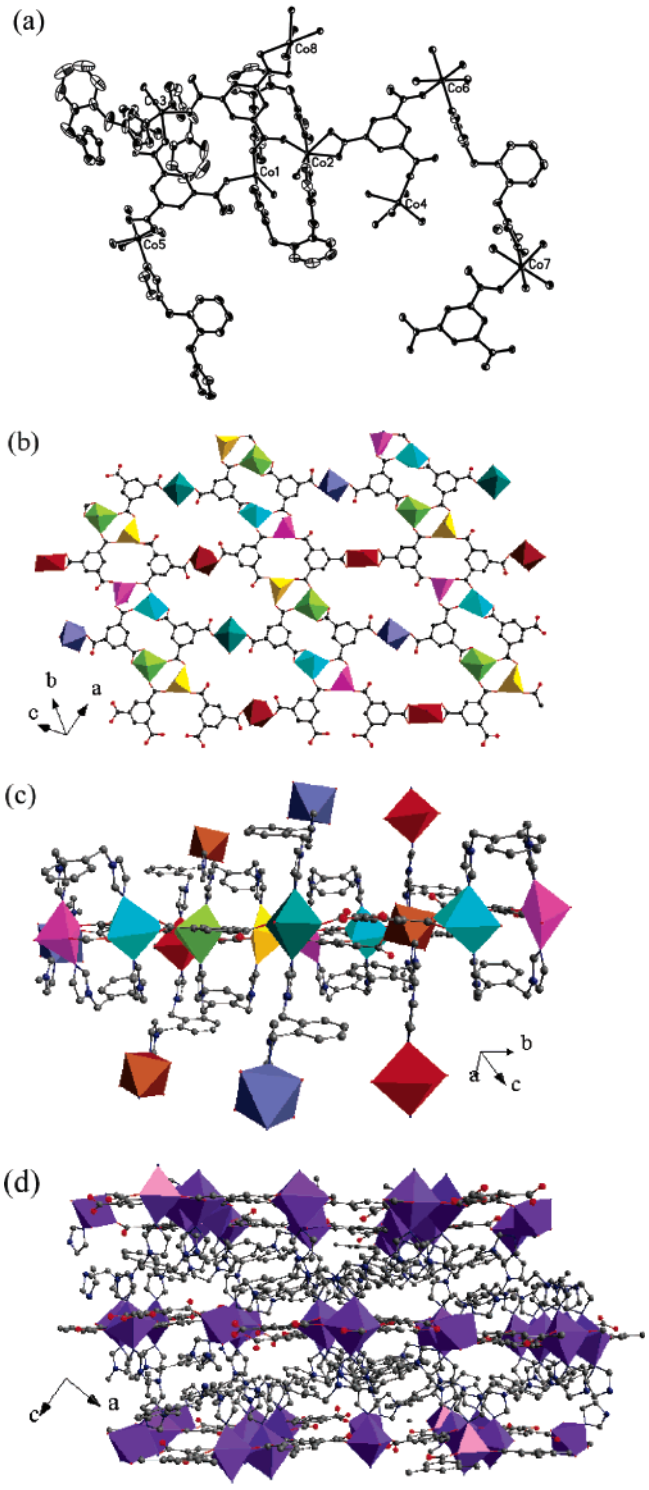

Figure 4. (a) ORTEP diagram showing the coordination environments for Co atoms in **4** at 30% probability. (b) Polyhedral representation of the cobalt−BTC 2D layer (gold and pink trigonal bipyramids represent Co1 and Co3 atoms; other octahedra represent Co2 (lime), Co4 (turquoise), Co5 (brown), Co6 (blue gray), Co7 (teal), and Co8 (red) atoms, respectively). (c) Coordination modes of L^1 ligands. (d) Polyhedral representation of the 3D metal−organic framework. (The guest water molecules and all of hydrogen atoms are omitted for clarity.)

centers are linked by two L^3 ligands and two BTC anions to give a 38-membered ring (C). Six zinc centers are connected by two L^3 ligands and four BTC anions to form a 54-membered ring (D). Rings A, B, and D are common arrangements which have been found in other transition metal complexes.[20]

If BTC anions are considered as four-connected nodes, the structure of **3** can be symbolized as a net with $(4\cdot6^2\cdot8^3)_2(8\cdot10^2)(4\cdot6\cdot8^3\cdot10)_2$ topology (Figures 3d and S12).[17]

Structure Description of 4. As shown in Figure 4a, the structure of **4** contains eight kinds of unique Co atoms, four kinds of unique BTC anions, and six kinds of unique L^1 ligands. Co1 and Co3 atoms are five-coordinate, and other cobalt atoms are six-coordinate. Each of Co1 and Co3 atoms is coordinated by three carboxylate oxygen atoms (Co−O 1.990(3)−2.065(3) Å) from three BTC anions and two nitrogen atoms (Co−N 2.117(4)−2.132(4) Å) from two L^1 ligands. Co2 and Co4 atoms are coordinated by four carboxylate oxygen atoms (Co−O 2.009(3)−2.293(3) Å) from three BTC anions and two nitrogen atoms (Co−N 2.087(4)−2.115(4) Å) from two L^1 ligands. Each of Co5, Co6, and Co7 atoms lies at an inversion center and is coordinated by two carboxylate oxygen atoms (Co−O 2.030(3)−2.111(3) Å) from two different BTC anions, two water molecules (Co−O 2.125(3)−2.190(3) Å), and two nitrogen atoms (Co−N 2.101(4)−2.158(5) Å) from two L^1 ligands. Co8 also lies at an inversion center and is coordinated by four carboxylate oxygen atoms (Co−O 2.107(3)−2.184(3) Å) from two BTC anions and two nitrogen atoms (Co−N 2.110(4) Å) from two L^1 ligands. All of the coordination bonds are within normal distances.[21]

The four unique BTC anions display two kinds of coordination modes (Chart 2b,c), and each of them coordinates to four cobalt atoms. Co^{II} centers are bridged by BTC anions to form a 2D Co−BTC polymeric network (Figure 4b). Six unique L^1 ligands of **4** show two kinds of conformations (Figure 4c). Two L^1 ligands adopt a trans-conformation,[13a,c] coordinating to two Co^{II} centers from adjacent Co−BTC layers. The other four display a cis-conformation as the L^1 ligands in compound **1** and two *cis*-L^1 ligands link two neighboring Co^{II} ions of the same Co−BTC polymeric layer to form a $[Co(L^1)_2Co]$ dimer (Figure S13). As depicted in Figure 4d, the 2D Co−BTC layers are connected by *trans*-L^1 ligands to form a 3D polymeric structure.

Structure Description of 5. As shown in Figure 5a, the structure of **5** contains two kinds of unique Co atoms. Co1 atom is coordinated by two carboxylate oxygen atoms (Co−O 1.976(4)−2.036(6) Å) from two BTC anions and two nitrogen atoms (Co−N 2.004(8)−2.030(6) Å) from two

(20) (a) Li, X. J.; Cao, R.; Bi, W. H.; Wang, Y. Q.; Wang, Y. L.; Li, X.; Guo, Z. G. *Cryst. Growth Des.* **2005**, *5*, 1651. (b) Ma, C.; Chen, C.; Liu, Q.; Liao, D.; Li, L.; Sun, L. *New J. Chem.* **2003**, *27*, 890. (c) Duan, L. M.; Xie, F. T.; Chen, X. Y.; Che, Y.; Lu, Y. K.; Cheng, P.; Xu, J. Q. *Cryst. Growth Des.* **2006**, *6*, 1101. (d) Hong, X. L.; Li, Y. Z.; Hu, H. M.; Pan, Y.; Bai, J. F.; You, X. Z. *Cryst. Growth Des.* **2006**, *6*, 1221.

(21) (a) Gong, Y.; Hu, C. W.; Li, H.; Tang, W. *Inorg. Chem. Commun.* **2006**, *9*, 273. (b) Zhang, G. Q.; Yang, G. Q.; Ma, J. S. *Cryst. Growth Des.* **2006**, *6*, 375. (c) Liu, F. C.; Zeng, Y. F.; Jiao, J.; Bu, X. H.; Ribas, J.; Batten, S. R. *Inorg. Chem.* **2006**, *45*, 2776.

Structure description of 5.

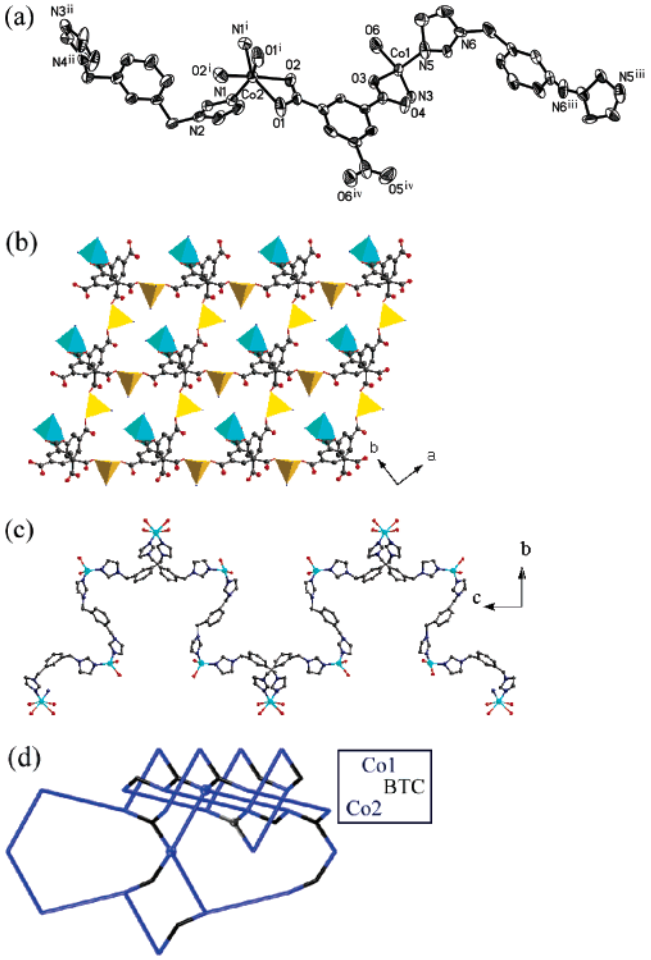

Figure 5. (a) ORTEP diagram showing the coordination environments for Co atoms in **5**. (b) Polyhedral representation of the 2D cobalt−BTC layer (turquoise octahedra represent Co1 atoms and gold tetrahedrons represent Co2 atoms; the guest water molecules and all of hydrogen atoms are omitted for clarity). (c) Infinite polymeric chain of L^2 ligands. (d) Schematic diagram (OLEX) showing the $(6^4{\cdot}8^2)_2(6^2{\cdot}8^2{\cdot}10^2)(6^3)_2$ network.

L^2 ligands, showing a tetrahedral geometry.[22] Co2 lies at an inversion center and is six-coordinated by four oxygen atoms from two BTC anions (Co−O 2.141(4)−2.225(6) Å) and two nitrogen atoms from two L^2 ligands (Co−N 2.051(6) Å). The coordination modes of the BTC anions in **5** are shown in Chart 2d, and each BTC anion coordinates to three Co atoms. The cobalt atoms are bridged by BTC anions to form a 2D network (Figures 5b and S14).

The coordination between cobalt centers and L^2 ligands results in a beautiful ruffling (Figure 5c). L^2 ligands also display two conformations as in compound **2**. One L^2 ligand shows a S-shaped conformation[15] with the Co···Co distance of 13.90(5) Å. The Co−BTC layers are connected through these S-shaped L^2 ligands to form a unique 3D network (Figure S15). The other L^2 adopts the C-shaped conformation,[16] with the Co···Co distance of 11.20(2) Å. The participation of these C-shaped L^2 ligands leads the formation of a complicated 3D structure.

If BTC anions are considered as three-connected nodes, the structure of **5** can be symbolized as a net with $(6^4{\cdot}8^2)_2(6^2{\cdot}8^2{\cdot}10^2)(6^3)_2$ topology (Figures 5d and S16).[17]

Structure Description of 6. As shown in Figure 6a, compound **6** consists of four kinds of unique Co atoms, two kinds of unique BTC anions, and three kinds of unique L^3 ligands. Each of the Co1 and Co2 atoms is six-coordinated by three oxygen atoms from BTC anions (Co−O 2.050(5)−2.218(4) Å), two μ_3-OH (Co−O 2.087(4)−2.110(5) Å), and one N atom from the L^3 ligand (Co−N 2.103(6)−2.100(5) Å). Co3 is six-coordinated by three oxygen atoms from three BTC anions (Co−O 2.053(4)−2.376(4) Å), one μ_3-OH (Co−O 2.023(4) Å), one water molecule (Co−O 2.283-(5) Å), and one N atom from the L^3 ligand (Co−N 2.125(5) Å). Co4 is five-coordinated by three oxygen atoms from three BTC anions (Co−O 2.010(5)−2.244(4) Å), one μ_3-OH (Co−O 1.987(5) Å), and one N atom from the L^3 ligand (Co−N 2.080(6) Å). The Co^{II} centers are connected by μ_3-OH and carboxylate O atoms to form two kinds of cobalt−oxygen clusters (Figure 6b). These cobalt−oxygen clusters have rarely been observed in the literature.[7b,23]

Each of the two unique BTC anions displays a μ-6 coordination mode as shown in Chart 2e. The cobalt−oxygen clusters are connected through BTC anions to form a 2D network (Figure 6c). Some L^3 ligands in **6** are bonded to the same Co−BTC polymeric layer; and the others are bonded to two adjacent layers (Figure S17). The latter further connect these 2D Co−BTC layers to form a 3D framework (Figure 6d).

Coordination of BTC Anions. According to previous studies, the reactions of BTC anion with Zn^{II} and Co^{II} produced $[Zn_3(BTC)_2(H_2O)_8]{\cdot}4H_2O$[12a] and $[Co_3(BTC)_2(H_2O)_{12}]$,[24] respectively. Both of the compounds contain two types of BTC anions. One type of BTC anion coordinates to three M^{2+} ions (Chart 2d), while the other coordinates to two M^{2+} ions (Chart 2f). Both the compounds exist as a corrugated chain. In compounds **1**−**6**, BTC anions show a variety of coordination modes, and several metal−BTC skeletons are formed (1D ladder, 2D layer, and 3D framework). In **1** and **2**, each BTC anion coordinates to three Zn^{II} centers (Chart 2a), and Zn^{II} centers are bridged by BTC anions to form a 1D ladder skeleton. In **3**, the BTC anions display two coordination modes (Chart 2b,c), and Zn^{II} centers are connected by BTC anions to form a complicated 3D framework. In **4**, the four unique BTC anions display the same coordination modes as in **3** (Chart 2b,c), and BTC anions link the Co^{II} centers to form a 2D polymeric layer. In **5**, each BTC coordinates to three Co^{II} centers (Charts 2d), and the cobalt centers are connected by BTC anions to form

(22) (a) Wei, C. H.; Dahi, L. F. *J. Am. Chem. Soc.* **1968**, *90*, 3969. (b) Rujiwatra, A.; Kepert, C. J.; Rosseinsky, M. J. *Chem. Commun.* **1999**, 2307. (c) Adams, R. D.; Bunz, U. H. F.; Fu, W.; Nguyen, L. *J. Organomet. Chem.* **1999**, *578*, 91. (d) Schneider, O.; Gerstner, E.; Weller, F.; Dehnicke, K. *Z. Anorg. Chem.* **1999**, *625*, 1101.

(23) (a) Liu, Y. L.; Na, L. Y.; Zhu, G. S.; Xiao, F. S.; Pang, W. Q.; Xu, R. R. *J. Solid State Chem.* **2000**, *149*, 107. (b) Harrison, W. T. A.; Gier, T. E.; Stucky, G. D.; Broach, R. W.; Bedard, R. A. *Chem. Mater.* **1996**, *8*, 145. (c) Fan, J.; Hanson, B. E. *Inorg. Chem.* **2005**, *44*, 6998.

(24) (a) Yaghi, O. M.; Li, H. L.; Grov, T. L. *J. Am. Chem. Soc.* **1996**, *118*, 9096. (b) Zhang, W. R.; Bruda, S.; Landee, C. P.; Parent, J. L.; Turnbull, M. M. *Inorg. Chim. Acta* **2003**, *342*, 193.

Structure description of 6.

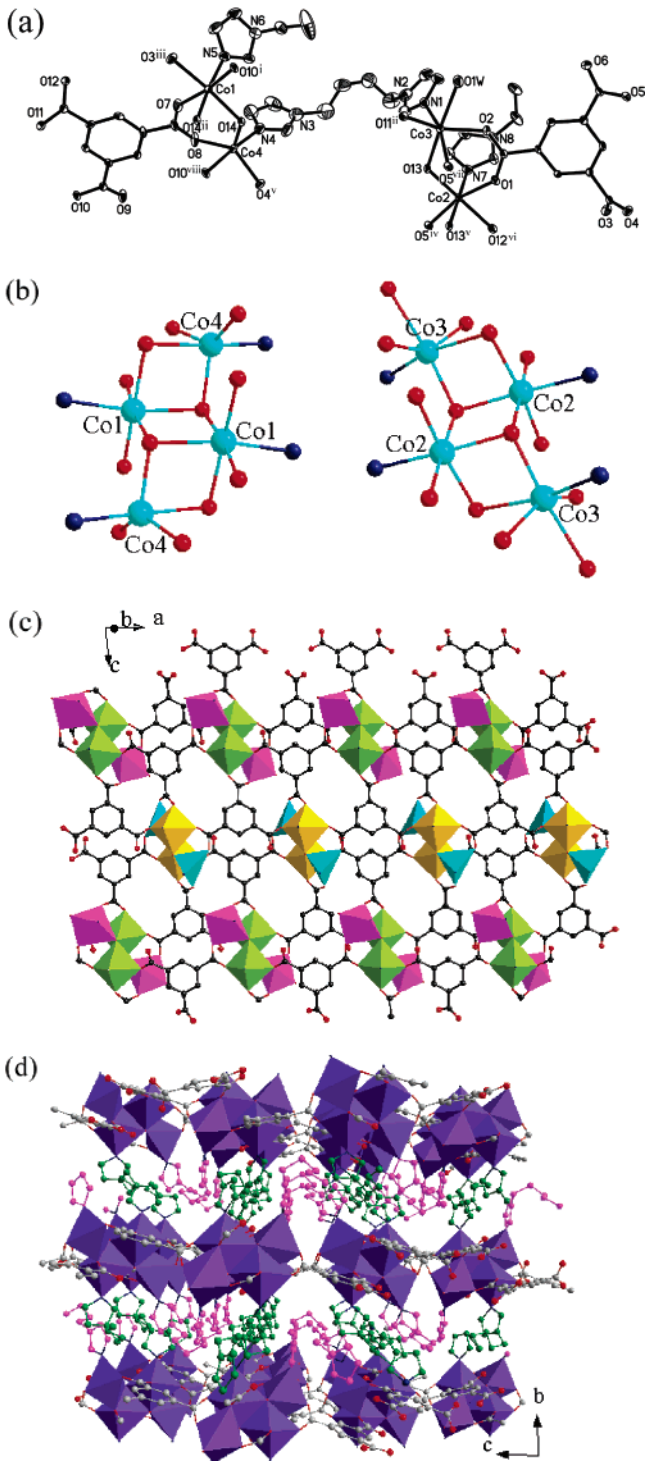

Figure 6. (a) ORTEP diagram showing the coordination environments for Co atoms in **6**. (b) Schematic drawing of the cobalt−oxygen clusters. (c) Polyhedral representation of the 2D layer connected by BTC anions (gold, lime, and pink octahedra represent Co1, Co2, and Co3 atoms, respectively; turquoise trigonal bipyramids represent Co4 atoms). (d) Polyhedral representation of the 3D metal−organic framework (pink L^3 represents the ligand bonded to the same layer, and green L^3 represents the ligand bonded to two adjacent layers). (The guest water molecules and all of hydrogen atoms are omitted for clarity.)

a 2D network. In **6**, two kinds of BTC anions display μ-6 coordination modes (Chart 2e), and the BTC anions link the Co−O clusters to form a 2D network.

Coordination of Bis(imidazole) Ligands. In this study, compounds **1**−**6** display a diversity of 2D and 3D frameworks, and the connectivities of the six compounds are strongly related to the bis(imidazole) ligands. As described above, the bis(imidazole) ligands serve as bridging ligands with two N atoms of the imidazole units coordinating to the metal atoms. In **1**, zinc centers are linked by L^1 ligands to form $[Zn(L^1)_2Zn]$ dimers; in **4**, both $[Co(L^1)_2Co]$ dimer and infinite $-Co-L^1-Co-L^1-$ chain are formed. In **2**, zinc centers are bridged by L^2 ligands to form zigzag chains and helices simultaneously; in **5**, L^2 ligands link cobalt centers to form a ruffling chain. In **3**, zinc centers are connected by L^3 ligands to form $[Zn(L^3)Zn]$ dimers; in **6**, Co−O clusters are connected by L^3 ligands to form a 2D network.

Effect of Metal Cations on the Framework. For **1** and **4**, the coordination numbers of Zn cations (4 and 6 with molar ratio of 2:1) are lower than those of Co cations (5 and 6 with molar ratio of 1:2), and the molar ratio of Zn to L^1 (3:2) in **1** is different from that of Co to L^1 (1:1) in **4**. The difference between the coordination numbers of Co and Zn is caused by the different molar ratios of M to L^1 and the different coordination modes of BTC anions simultaneously. This results in the structural changes from 2D of **1** to 3D of **4**. For **2** and **5**, the coordination numbers of Zn cations (4) are lower than those of Co cations (4 and 6 with molar ratio of 1:1). Since the frameworks of **2** and **5** have the same component of $M_3(BTC)_2(L^2)_3$, the difference between the coordination numbers of Co and Zn is caused by the different coordination modes of BTC anions. And this finally results in two different 3D frameworks of **2** and **5**. Unlike **3**, in addition to BTC anions, **6** contains μ_3-OH anions. The Co cations in **6** are bridged by μ_3-OH anions to form $[Co_4(\mu_3\text{-}OH)_2]^{6+}$ units whose coordination behavior is much different from that of the Zn cations of **3**. And this results in the changes of the coordination modes of BTC anions and, finally, causes the difference between the frameworks of **3** and **6**.

As discussed above, BTC anions show a variety of coordination modes as polydentate bridging ligands (Chart 2), and the bis(imidazole) ligands act as bidentate bridging ligands with different conformations. The simultaneous use of the bis(imidazole) ligands and BTC ligands affords various architectures of **1**−**6**. Many factors, such as the stoichiometric ratio of the components, the radii of metal ions, the versatility of the metal coordination geometries, and the donor characters of nitrogen and oxygen atoms to the metals, play fundamental roles in the formation of the final products. Since these factors work together to affect the structures, it is difficult to separate and rationalize them and it is hard to propose definitive reasons as to why each compound adopts a different configuration with our present state of knowledge.

Thermal Analysis. To characterize the compounds more fully in terms of thermal stability, their thermal behaviors were studied by TGA (Figures S18 and S19 in the Supporting information). The experiments were performed on samples consisting of numerous single crystals of **1**−**6** under N_2 atmosphere with a heating rate of 10 °C/min.

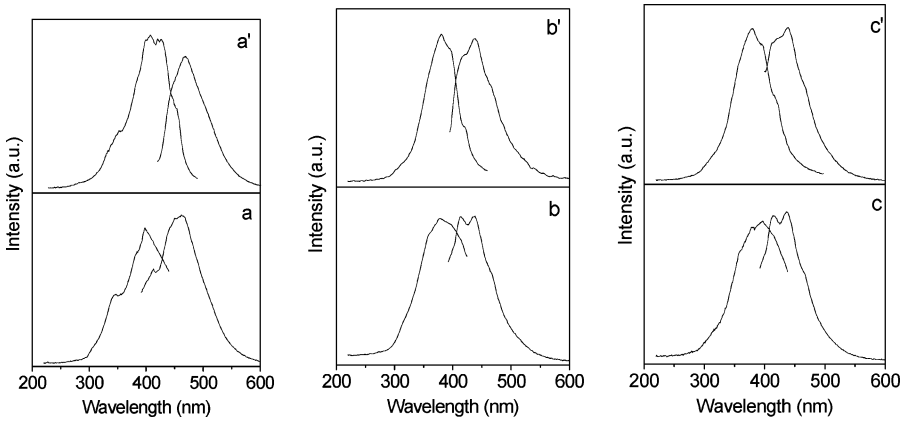

Figure 7. Solid-state photoluminescent spectra of (a) **1**, (b) **2**, and (c) **3** and free ligands (a′) L^1, (b′) L^2, and (c′) L^3 at room temperature.

For compound **1**, the weight loss corresponding to the release of water molecules is observed from room temperature to 230 °C (obsd 10.1%, calcd 10.40%). The anhydrous compound begins to decompose at 328 °C. Compound **2** is stable up to 335 °C, where the framework structure begins to collapse. For **3**, the weight loss attributed to the gradual release of water molecules is observed in the range 35−147 °C (obsd 5.0%, calcd 3.87%). The destruction of the anhydrous compound occurs from 290 to 560 °C, leading to the formation of zinc oxide as the residue (obsd 25.6% calcd 26.21%). The TGA curve of **4** shows that it undergoes dehydration in the range of 35−170 °C (obsd 6.8%, calcd 7.64%). The decomposition of the anhydrous compound occurs at 332 °C. Compound **5** lost its water molecules from 35 to 94 °C (obsd 0.8%, calculated 0.68%). The anhydrous $Co_{1.5}(BTC)(L^2)_{1.5}$ was stable up to 350 °C, and the removal of organic components occurs from 350 to 610 °C. For compound **6**, the weight loss in the range of 35−203 °C corresponds to the departure of water molecules (obsd 7.4%, calcd 8.52%). The removal of the organic components occurs in the range of 320−665 °C. The remaining weight corresponds to the formation of Co_2O_3 (obsd 28.5%, calcd 28.51%).

Luminescent Properties. The solid-state photoluminescent spectra of **1**−**3** and the neutral ligands L^1−L^3 are depicted in Figure 7. Compound **1** shows a main peak at 463 nm with a shoulder at 413 nm upon excitation at 397 nm. Compounds **2** and **3** exhibit two intense emission maxima at 414 and 438 nm for **2** and 415 and 436 nm for **3** upon excitation at 397 nm, respectively. The main emission peaks of L^1−L^3 are at 468, 440, and 438 nm, respectively. The peaks at 463, 438, and 436 nm of compounds **1**−**3** are probably due to $\pi^* \rightarrow \pi$ transitions of neutral ligands because similar peaks also appear for the free bis(imidazole) ligands, respectively.[25] The peaks of 413, 414, and 415 nm for the compounds exhibit a red-shift with respect to the free H_3-BTC (380 nm, $\lambda_{ex} = 334$ nm),[9e,f] which may be assigned to the intraligand fluorescent emission of BTC.[9c,26] The N-donors ligand and O-donors ligand show contribution to the fluorescent emission of the three compounds simultaneously.

Magnetic Properties. The temperature-dependent magnetic susceptibility data of compounds **4**−**6** have been measured for polycrystalline samples at an applied magnetic field of 1000 Oe in the temperature range of 2−300 K (Figure 8). For **4**, the $\chi_m T$ value at 300 K is 12.89 $cm^3\ mol^{-1}$ K (10.15 μ_B), which is slightly higher than the value expected[27] for four uncoupled high-spin Co^{II} centers (Figure 8a). As T is lowered, $\chi_m T$ decreases smoothly to a value of 10.89 $cm^3\ mol^{-1}$ K at 38 K. On further cooling, $\chi_m T$ goes up to a maximum value of 11.65 $cm^3\ mol^{-1}$ K at 22 K and then goes down quickly to a minimum value of 5.47 $cm^3\ mol^{-1}$ K at 2 K. The decrease of $\chi_m T$ at high temperature is a typical manner of spin−orbit coupling, and it is mainly due to the single-ion behavior of Co^{II}.[28] The increase of $\chi_m T$ between 38 to 22 K is due to the ferromagnetic coupling within the carboxylate-bridged Co^{II} ions.[29] The magnetic susceptibility above 40 K obeys the Curie−Weiss law with the Curie constant $C = 13.21$ $cm^3\ mol^{-1}$ K and the Weiss constant $\Theta = -11.11$ K.

Compound **5** exhibit similar magnetic behavior with compound **4** (Figure 8b). For **5**, the $\chi_m T$ value at 300 K is 3.83 $cm^3\ mol^{-1}$ K (5.53 μ_B), which is consistent with the expected value (3.75 $cm^3\ mol^{-1}$ K, 5.48 μ_B) of two isolated $S = 3/2$ spin-only Co^{II} ions ($g = 2.0$). As T is lowered, $\chi_m T$ decreases smoothly to a value of 3.50 $cm^3\ mol^{-1}$ K at 48 K. On further cooling, $\chi_m T$ goes up to a maximum value of 4.35 $cm^3\ mol^{-1}$ K at 22 K and then goes down quickly to a minimum value of 2.53 $cm^3\ mol^{-1}$ K at 2 K. The decrease of $\chi_m T$ at high temperature does not imply antiferromagnetic coupling between Co^{II} ions, as it is mainly due to the single-ion behavior of Co^{II}.[28] The increase of $\chi_m T$ between 44 to 22 K is due to the ferromagnetic coupling within the

(25) (a) Shi, X.; Zhu, G.; Fang, Q.; Wu, G.; Tian, G.; Wang, R.; Zhang, D.; Xue, M.; Qiu, S. *Eur. J. Inorg. Chem.* **2004**, 185. (b) Zhang, X. M.; Tong, M. L.; Gong, M. L.; Chen, X. M. *Eur. J. Inorg. Chem.* **2003**, 138. (c) Tian, G.; Zhu, G. S.; Fang, Q. R.; Guo, X. D.; Xue, M.; Sun, J. Y.; Qiu, S. L. *J. Mol. Struct.* **2006**, *787*, 45.

(26) (a) Thirumurugan, A.; Natarajan, S. *J. Chem. Soc., Dalton Trans.* **2004**, 2923. (b) Chen, Z. F.; Xiong, R. G.; Zhang, J.; Chen, X. T.; Xue, Z. L.; You, X. Z. *Inorg. Chem.* **2001**, *40*, 4075.

(27) Telfer, S. G.; Kuroda, R.; Lefebvre, J.; Leznoff, D. B. *Inorg. Chem.* **2006**, *45*, 4592.

(28) (a) Sun, H. L.; Gao, S.; Ma, B. Q.; Su, G. *Inorg. Chem.* **2003**, *42*, 5399. (b) Sun, H. L.; Wang, Z. M.; Gao, S. *Inorg. Chem.* **2005**, *44*, 2169.

(29) Zhang, Y. Z.; Tong, M. L.; Zhang, W. X.; Chen, X. M. *Angew. Chem., Int. Ed.* **2006**, *45*, 6310.

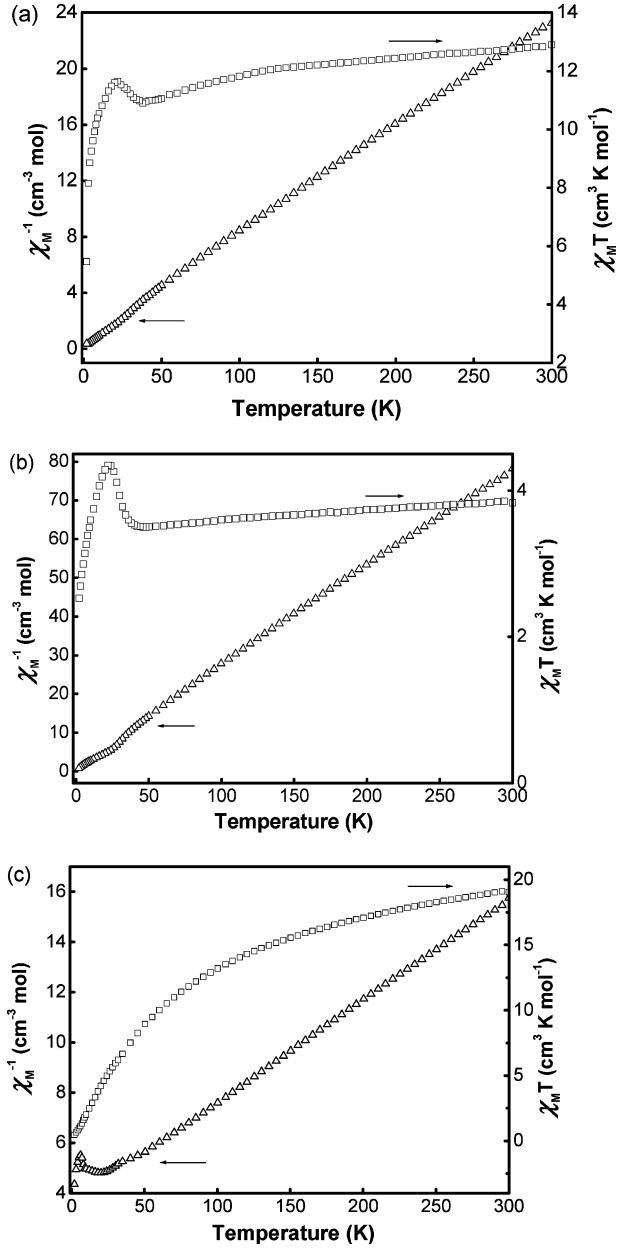

Figure 8. Plots of the temperature dependence of $\chi_m T$ (open squares) and χ_m^{-1} (open triangles) for compounds (a) **4**, (b) **5**, and (c) **6**.

carboxylate-bridged Co^{II} ions.[29] The magnetic susceptibility in the range of 48−300 K obeys the Curie−Weiss law with $C = 3.94$ cm^3 mol^{-1} K and $\Theta = -9.52$ K.

For **6**, the $\chi_m T$ value at 300 K is 19.05 cm^3 mol^{-1} K (12.34 μ_B, Figure 8c), far larger than the theoretic value[27] for four spin-only Co^{II} ions, indicating the unquenched orbital contribution of Co^{II} ions. Upon cooling of the sample, the values of $\chi_m T$ keep smoothly decreasing in 300−2.0 K range, indicating an overall antiferromagnetic coupling in compound **6**.[30] The magnetic susceptibility above 45 K can be well fit to Curie−Weiss law with $C = 24.73$ cm^3 mol^{-1} K and $\Theta = -88.63$ K. The negative Θ value further confirms the presence of antiferromagnetic interaction in **6**.

Conclusion

The simultaneous use of the flexible bis(imidazole) ligands and aromatic BTC anions to react with zinc and cobalt metals affords six interesting polymeric architectures, illustrating again the aesthetic diversity of coordinative network chemistry. The results of this study not only illustrate that the coordination modes of carboxylate ligands and the nature of the neutral ligands play an important role in the construction of coordination polymers but also give a nice example of the metal-controlled polymeric architecture construction. It is anticipated that more metal complexes containing neutral ligands and carboxylate anions with interesting structures as well as physical properties will be synthesized.

Acknowledgment. We thank the National Natural Science Foundation of China (Grant No. 20471014), Program for New Century Excellent Talents in Chinese University (Grant NCET-05-0320), the Fok Ying Tung Education Foundation, the Science Foundation for Young Teachers of NENU (Grant No. 20070314), and the Analysis and Testing Foundation of Northeast Normal University for support.

Supporting Information Available: Six X-ray crystallographic files (CIF), selected bond distances and angles, simulated and experimental powder XRD patterns, structure illustrations, and TGA curves of compounds **1**−**6** and the closed circuit environment around each node for compounds **2**, **3**, and **5**. This material is available free of charge via the Internet at http://pubs.acs.org.

IC061575L

(30) (a) Langley, S. J.; Helliwell, M.; Sessoli, R.; Rosa, P.; Wernsdorfer, W.; Winpenny, R. E. P. *Chem. Commun.* **2005**, 5029. (b) Akine, S.; Dong, W. K.; Nabeshima, T. *Inorg. Chem.* **2006**, *45*, 4677. (c) Sun, H. L.; Gao, S.; Ma, B. Q.; Batten, S. R. *CrystEngComm* **2004**, *6*, 579. (d) Angelov, S.; Drillon, M.; Zhecheva, W.; Stoyanova, R.; Belaiche, M.; Derory, A.; Herr, A. *Inorg. Chem.* **1992**, *31*, 1514.